



## Static and modal numerical analyses for the roof structure of a railway freight refrigerated car

Raffaele Sepe

*Dept. of Chemical, Materials and Production Engineering, University of Naples Federico II P.le V. Tecchio, 80 - 80125 Naples, Italy. raffsepe@unina.it*

Angela Pozzi

*Advanced Transports s.r.l., Zona Ind Ex Indesit, - 81030 Gricignano di Aversa, Italy. angela.pozzi@advancedtransports.it*

---

**ABSTRACT.** Numerical analyses by finite element method and experimental tests are used to determine static and dynamic behaviour of railway vehicles. Experimental measurements are very time consuming and expensive, so they cannot be used at all stages of design. Numerical simulations do not have the disadvantages of experimental methods, but it is necessary to verify them by experiments to obtain realistic results. Full-width/full-length, half-width/full-length and half-width/half-length modeling approaches can be used to determine static and vibrational behaviours of railway vehicles depending or not on the symmetry of roof structure and applied load. Different static loading cases defined in standards such as EN 12663, UIC CODE OR 577 and ERRI B12/RP17 have to be considered in FE analyses. Evaluation of stress states, buckling and vibrational behaviours for a roof structure of a railway freight refrigerated car are presented. To highlight the vibrational behaviour of the structure normal mode (free vibration) analyses are performed. As a result of the relevant simulations, structural characteristics and structural weaknesses of the design are determined.

**KEYWORDS.** Railway freight car; Refrigeration system; Finite Element Method (FEM).

---

### INTRODUCTION

The railway vehicle must meet a number of requirements, including: safety requirements for crash scenarios, derailment, fire, pressure waves in tunnels, etc. The car body must also be within the specific construction profile of the operated line. It must be strong enough not to fail during typical maximum loads or during cyclic loading. A large amount of these requirements are, for example, covered by the standards EN 12663-1 and EN 12663-2 [1-2]. Static and dynamic tests are performed according to international standards [1-4] during the certification procedures of the railway vehicle before putting it into the service. Experimental measurements are very time consuming and expensive, so they cannot be used at all stages of design. Hence, today numerical methods are important tools in static and dynamic analyses of railway vehicles. In fact, numerical simulations do not have in same amount the aforementioned disadvantages of experimental methods. Finite Element Method (FEM) is a powerful numerical engineering analysis tool, hence widely used in static and dynamic stress analyses of railway vehicles, moreover, it can be used easily for different load cases and in all step of design due to its economy and flexibility.

---



To obtain static structural behaviour of the railway vehicles, i.e., stress and strain distribution, different static loading cases defined in standards such as UIC CODE OR 577 and ERRI B12/RP17 [3-4] can be used in FE analyses.

In recent years there has been an increased effort to investigate and improve the crashworthiness of passenger and freight rail vehicles by using FEM simulation. Several approach can be used to investigate the crashworthiness: simplified one-dimensional models can be used to evaluate interactions between vehicles.

Kirkpatrick et al. [5] presented a comparison of the various experimental, analytical, and computational approaches to evaluate rail vehicle crashworthiness. The experimental approaches include static and dynamic testing of vehicles and components using scale model and full-scale structures. Similarly, a wide range of analyses were performed to evaluate various aspects of rail vehicle crashworthiness.

Lewis et al. [6] describe development work in the area of crashworthiness of railway vehicles carried out during a four year period in the UK. Specific areas of investigation include vehicle overriding and the collision behaviour of complete trains or rakes of vehicles.

Hosseini-Tehrani and Bayat [7] conducted a systematic study to examine possible strategies to design a crashworthy ladder frame for the passenger train that behaves well under frontal impact conditions. For this purpose, various combinations of triggers and energy absorber members in one end of a ladder frame are studied and the improved design is proposed.

Caputo et al. [8] analyse the global crash behaviour of a railway vehicle involved in an accident to characterize the possible deformations, the kinematics and the dynamics behaviour of interiors and passengers. Such analyses are necessary to determine the biomechanical indexes to characterize the passive safety performance of the interior components.

Caputo et al [9-10] moreover study the causes and the typologies of secondary impact injuries suffered by passengers of a railway vehicle during a crash event. In particular, the installation of seatbelt has been investigated as a suitable system to restrain the passengers and different structural analyses of the seat, by means of finite element simulations, have been undertaken to determine if a stiffening of the seat is required to sustain those overloads. The MADYMO® code has been adopted to perform the preliminary MultiBody (MB) analyses which are required to calibrate and to evaluate the relevant parameters of dummy-seat contact surfaces and of seat-belt stiffness, while LS DYNA® code has been used for the structural dynamic FE analyses.

Lamanna and Sepe [11] analyse the energy absorbing capability of dedicated structural components made of a carbon fiber reinforced polymer and an emulsion polymerised styrene butadiene rubber. Static and dynamic numerical analyses are performed and numerical results are compared with experimental ones in terms of mean crushing forces, energy and peak crushing.

In this study are presented evaluations of static stress states, buckling and vibrational behaviours for an innovative roof structure of a railway freight refrigerated car. The global trading of perishable goods is possible thanks to product refrigeration and atmospheric control during transportation. The refrigerated railway freights are subject to very severe performance requirements because of the need to carry an enormous variety of cargoes under wide variations of climatic conditions and, as refrigerated transportation has increased, there has been substantial interest in improving energy consumption by reducing weight, and improving insulation and distribution system [12]. One of the aims of this paper is to describe the engineering development of a refrigerated railway freight car for transporting of goods and to evaluate the stress states under different static loading cases defined in standards such as EN 12663, UIC CODE OR 577 and ERRI B12/RP17. As a result of the relevant simulations, structural characteristics and structural weaknesses of the design are determined.

## **RAILWAY “GABS” FREIGHT REFRIGERATED CAR**

A railway standard freight car called “GABS” used by Austrian Federal Railways (German: Österreichische Bundesbahnen, ÖBB), Hungarian State Railways (Hungarian: Magyar Államvasutak, MÁV), National Society of French Railways (Société nationale des chemins de fer français SNCF) and National society of Italian railways “Trenitalia” was examined in this study.

The GABS car is being used Europe-wide. Various batches of this car with different doors and roofs have been produced over the time, and lots of different liveries have been realized. Principal GABS freight car dimensions are shown in Fig. 1. The wagon is used for the carriage of packed and other goods requiring protection against atmospheric impact, with the exception of animals and loose goods.

The wagon allows the introduction of mechanization in loading and unloading activities. The skeleton of the body is a welded structure composed of rolled and shaped metals. The wall covering of the body consists of water-resistant plywood, 15 mm thick for the side walls and 25 mm for the front walls.



The floor is built from softwood. On every side of the wagon there are two mobile doors, with a clearance of  $4000 \times 2150 \text{ mm}^2$ , as well as eight ventilation openings. Tab. 1 shows some typical specifications for a standard freight “GABS” car.

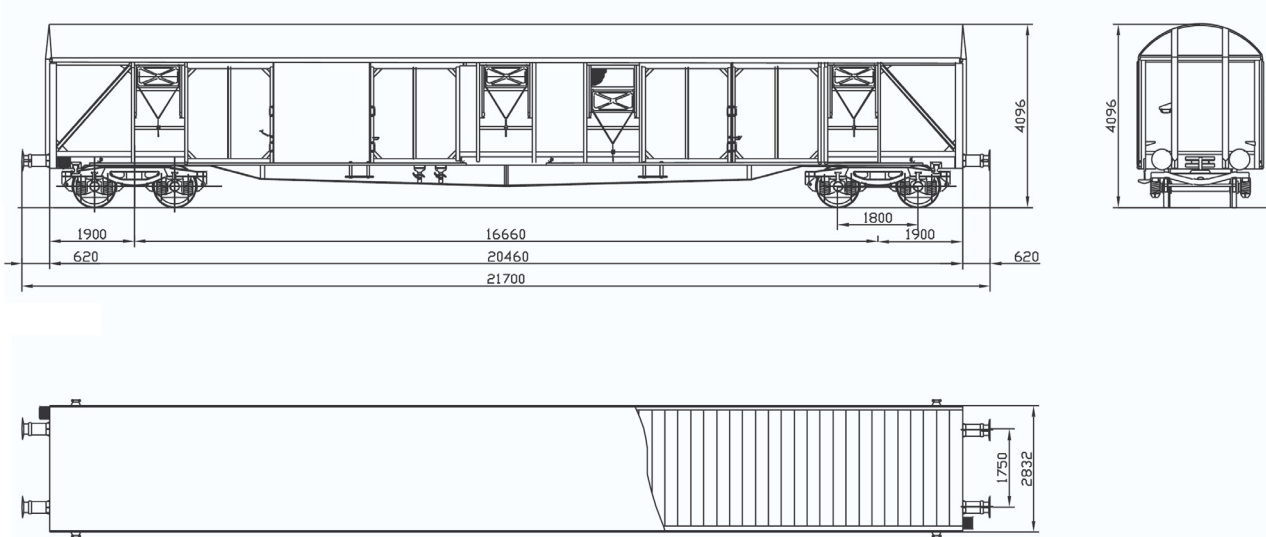


Figure 1: Dimension of a standard freight “GABS” car.

Type reference	GABS
Type number	1811–1812
Number of axles	4
Wheel base, distance between bogie pins [m]	16.66
Max. length over buffers [m]	21.70
Own weight [kg]	27500
Loading length [m]	20.39
Loading width [m]	2.57
Loading height [m]	2.77
Loading area [m <sup>2</sup> ]	53.00
Loading space [m <sup>3</sup> ]	137.00

Table 1: Typical specifications for a standard freight “GABS” car.

A standard freight “GABS” car was retrofitted in a refrigerated freight car. The reconstruction of wagons included: removal of the roof and preparation for welding (cutting and removal of upper construction, floor, sandblasting and cleaning), treatment and reinforcing the frame (frame straightening, welding steel reinforcements on the main longitudinal members, fixing and welding cross bearers and walking sheets, restoring headstocks), wagon revision (bogies, brakes and general revision), final assembly (final welding components and installation of a new roof and insulating panels), corrosion protection of the frame, final painting, sealing and assembly of the refrigeration system. The refrigeration system is composed of refrigeration units, installed into the structure of car, electrically driven by a generator joined to the wheel axes. Four lithium ion batteries are charged by sixty solar panels located on the roof of the car; moreover, the freight car is equipped with Phase Change Material (PCM) pipes which are installed in the roof of the car. During periods of insufficient lighting or when the car is standing in the station, batteries provide electricity to a classic refrigeration unit and the liquid eutectic collaborates providing refrigeration to the goods.



## FINITE ELEMENT MODEL OF THE ROOF OF THE FREIGHT REFRIGERATED CAR

The structure of the roof is shown in Fig. 2. The roof is composed of five identical modules connected to the upper longitudinal members of the structure of the wagon.

Each module has five ribs, connected by longitudinal elements, which support PCM pipes. The module is joined to the side members by means of elements which allow free deformations of the structure of the module in the transversal direction.

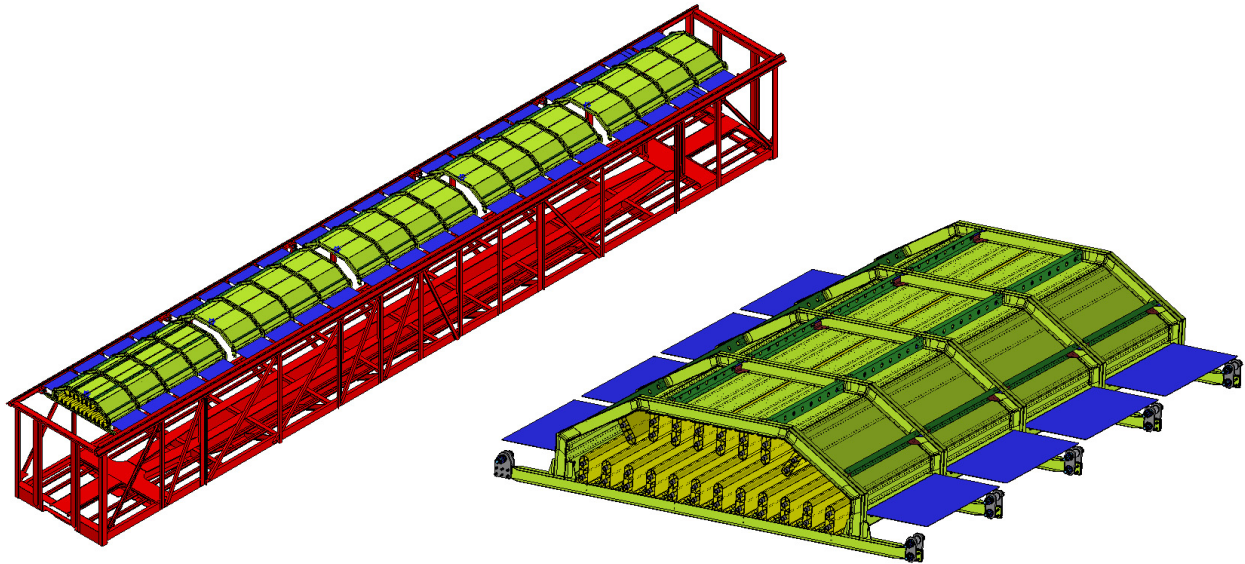


Figure 2: Structure of the roof of the freight car.

### *Description of the structure of the roof*

A single module is shown in Fig. 2. The principal frame of the roof module consist of "C" or "double T" sections, in both transverse and longitudinal direction (Fig. 3), there are also reinforcing plates between pairs of facing bars (Fig. 4); the structure is moreover covered by sheets and supports the pipes containing the PCM (Fig. 5).

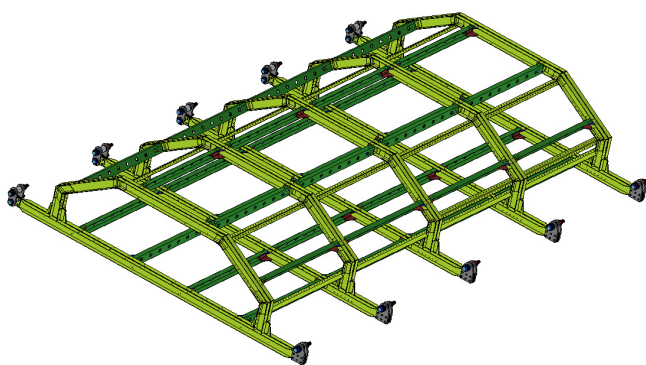


Figure 3: Principal frame of the roof module.

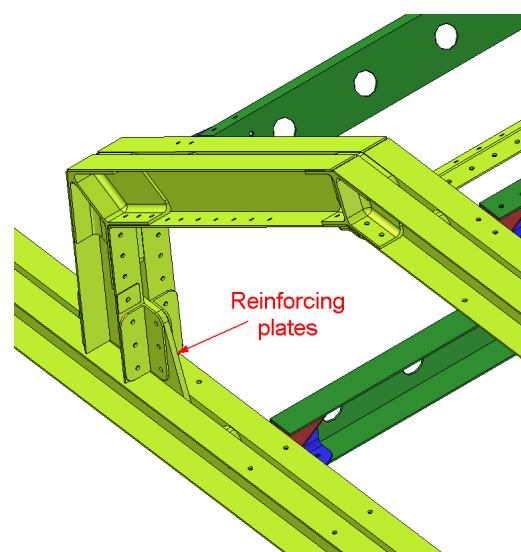


Figure 4: Reinforcing plates.

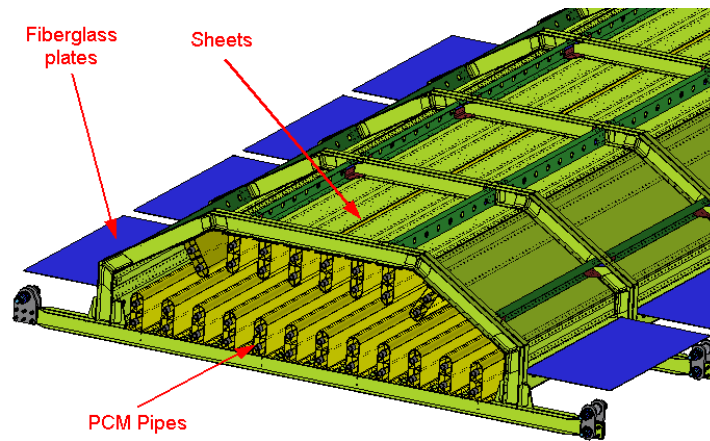


Figure 5: Position of sheets and PCM pipes in the roof.

### Materials

The structure of the roof is mainly made of five different materials.

- Sections ("C" or "double T"), made in Al 6061 T6 aluminium alloy;
- Sheets, made in Al 2024 T3 aluminium alloy;
- Plates, made in Al 7075-T651 aluminium alloy;
- Elements of constraint (hinges and pendulums), made in Al 2024 T351 aluminium alloy;
- Connection panel sides, made of fiberglass.

The mechanical properties of metallic materials are listed in Tab. 2.

Material	Density [kg/m <sup>3</sup> ]	E [MPa]	$\nu$	$\sigma_y$ (R 0.2%) [MPa]	$\sigma_u$ [MPa]
Al 6061 T6	2700	70000	0.33	240	260
Al 2024 T3	2700	70000	0.33	290	435
Al 7075 T651	2700	70000	0.33	360	400
Al 2024 T351	2700	70000	0.33	290	440
Fiberglass	1600	35000	0.33	40	60

Table 2: Mechanical properties of materials.

In Tab. 3 are reported the masses of structure, PCM pipes and insulating panels.

Component	Mass [kg]
Plates and frames	36
Sheets	94
Pipes	270
PCM	440
Insulating panels	85

Table 3: Mass of the components of the roof module.





### *FEM model*

To obtain the best balanced accuracy and efficiency in numerical simulations, standard convergence tests are applied. By using different mesh refinement levels, stresses in the critical regions are computed and an acceptable mesh refinement level is determined. The final container FE model is composed of 428,622 SHELL63 and 6,928 SOLID45 (ANSYS code), for a total of 435,550 elements and 449,556 nodes. Plates, sheets, pipes and the cross members which support them, are discretized with SHELL63 elements (four-node with six degrees of freedom at each node). The joint plates are discretized uniformly with hexahedral elements SOLID45 (eight-node with three translational degrees of freedom at each node). In addition, 160,188 rigid connection elements are used to represent fasteners in freight car FE model. Fig. 6 and 7 show the roof module mesh made of the aforesaid shell and solid elements.

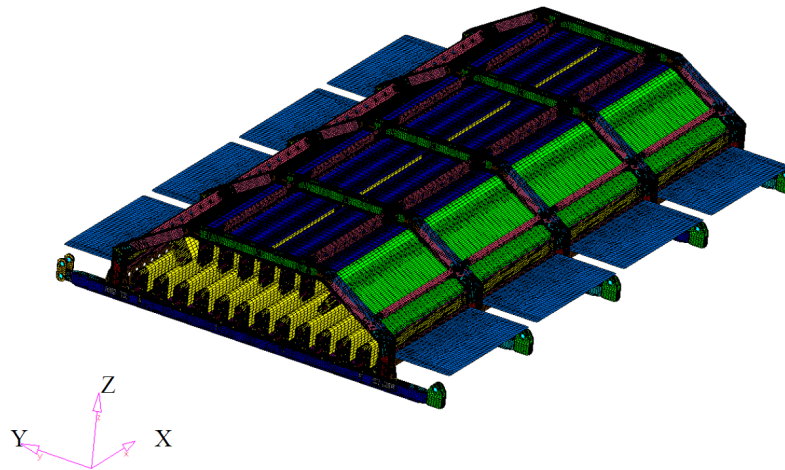


Figure 6: Roof module mesh.

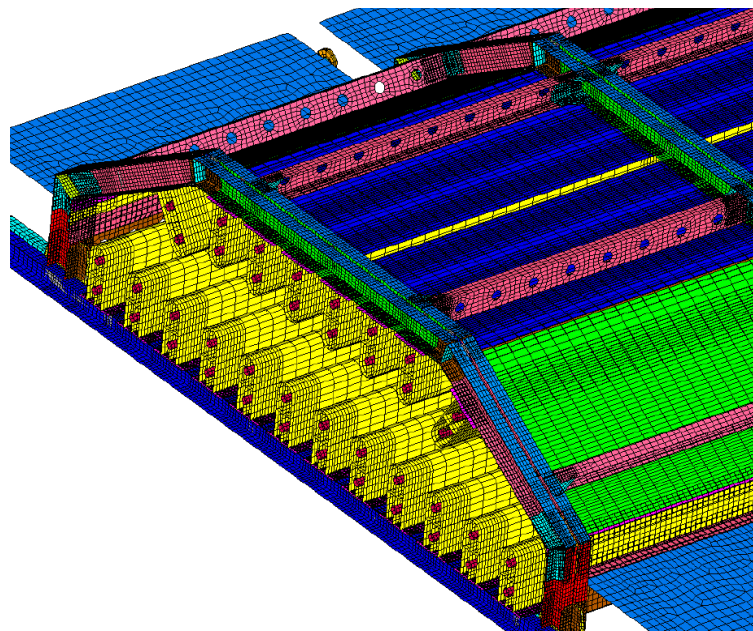


Figure 7: Roof module mesh (detailed view).

### *Loading and boundary conditions*

To obtain static structural behaviour of the roof structure, EN 12663, UIC CODE OR 577 and ERRI B12/RP17 standards are used. Railway vehicles are subjected to different loading scenarios in these standards such as symmetrical compression force and tensile force. According to these standards, loading and boundary conditions are adapted to FE simulations. In Tab. 4 and 5 are shown static and fatigue loading cases used in FE simulation.



Loading cases	Loading direction	Value
1	Vertical axis (Z)	$g_z = g$
2	Longitudinal axis (X)	$g_x = 5 g$
3	Transversal axis (Y)	$g_y = g$
4	Vertical axis (Z)	$g_z = 3 g$
5	Vertical and longitudinal axes	Loading 1 and 2
6	Vertical and transversal axes	Loading 1 and 3

Table 4: Static loading cases.

Loading cases	Loading direction	Value
7	Longitudinal axis (X)	$g_x = \pm 0.3 g$
8	Transversal axis (Y)	$g_y = \pm 0.4 g$
9	Vertical axis (Z)	$g_z = 1.3 g$
10	Vertical axis (Z)	$g_z = 0.7 g$

Table 5: Fatigue loading cases.

The roof module structure is joined to the side members of the wagon by two types of joints: a simple cylindrical joint on a side (Fig. 8) and a double cylindrical joint on the other side (Fig. 9); using this scheme the structure of the roof module can freely deform along the transversal direction.

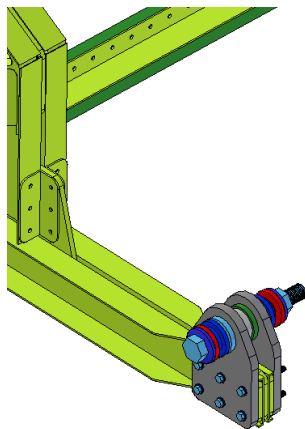


Figure 8: Simple cylindrical joint.

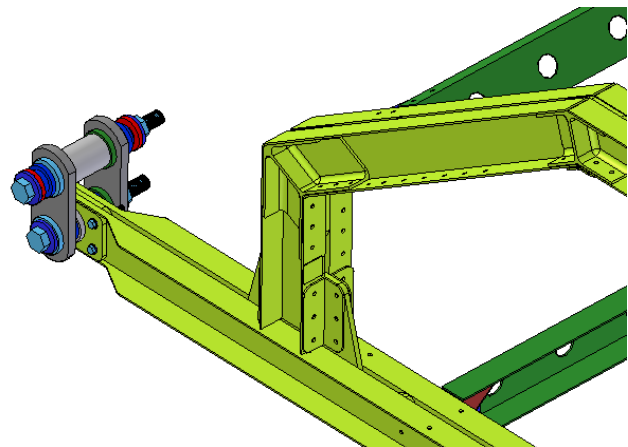


Figure 9: Double cylindrical joint.

Full width/full-length, half-width/full-length and half-width/half-length modeling approaches can be used to determine static and fatigue behaviours of railway vehicles depending or not on the symmetry of roof structure, loads and on particularity of phenomenon.

Analyzing loading and boundary conditions, it is possible to define two planes of symmetry for the problems:

- Middle plane YZ: this type of symmetry is valid for transversal loads (Y), vertical (Z) and their combinations.
- Middle plane XZ: this type of symmetry is valid for longitudinal loads (X), vertical (Z) and their combinations.



## STATIC AND FATIGUE LOADING RESULTS AND DISCUSSION

Three-dimensional finite element analyses have been carried out, based on the models and physical properties introduced above. Static analysis consisted of two stages, the initial concept design was analyzed in the first stage, then the structure was modified (the thickness of "C" or "double T" sections was changed from 2.5 mm to 3.0 mm) and simulated again under the same conditions in the second stage. As a result of the modifications, the roof module structure with better static strength properties was obtained (Tab. 6). The stress distributions and displacements were computed and analysed; details of the stress distributions of the modified roof module of some loading case will be shown.

Fig. 10 and 11 show deflection (mm) in vertical (Z) direction and the von Mises stress due to loading case 2 for the modified freight car structure. The deformed shape is symmetrical with respect to transversal (YZ) plane. The maximum displacement (load case 2) is 0.3 mm on the transversal principal frames.

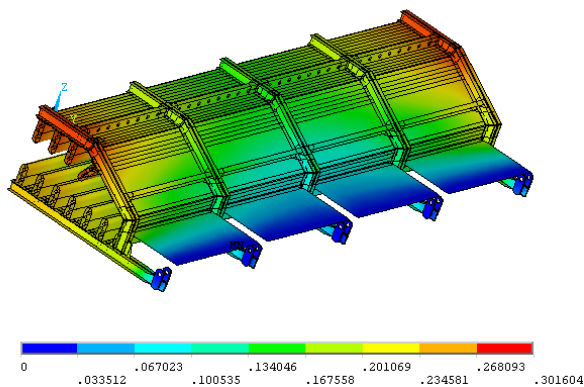


Figure 10: Deflection (mm) in (Z) direction due to loading case 2.

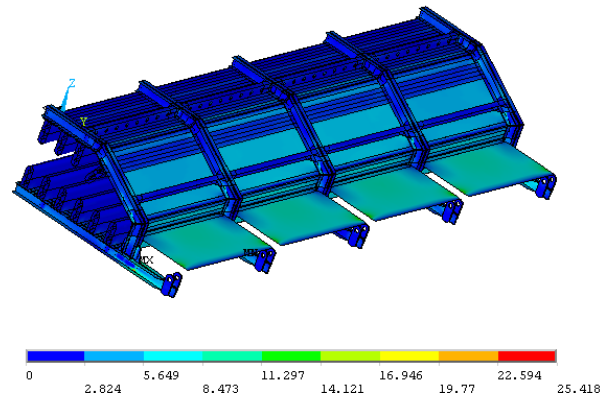


Figure 11: Von Mises stress (MPa) due to loading case 2.

Fig. 12 and 13 show deflection in a vertical (Z) direction and the von Mises stress due to loading case 4. The maximum displacement (load case 4) in vertical (Z) direction is 2.1 mm on the PCM pipes. The deformed shape is symmetrical with respect to longitudinal (XZ) plane.

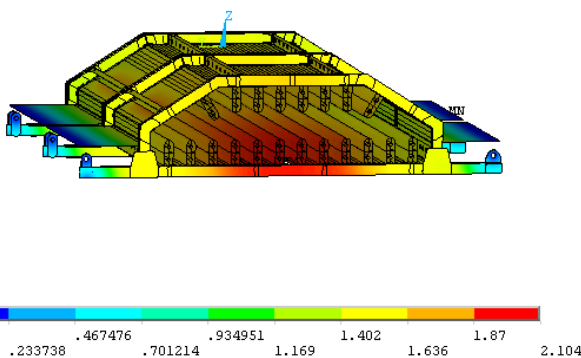


Figure 12: Deflection (mm) in (Z) direction due to loading case 4.

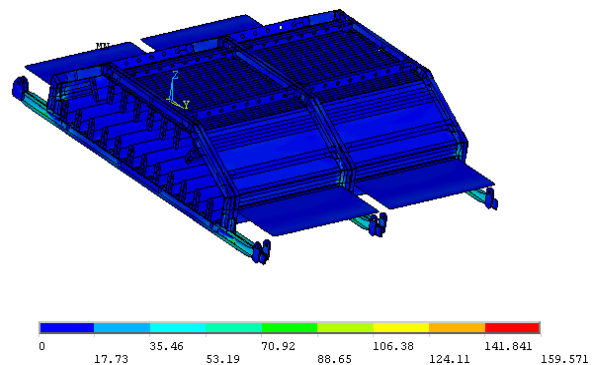


Figure 13: Von Mises stress (MPa) due to loading case 4.

The maximum value (159.6 MPa) of the stress was found in the transversal frame at the intersection of an uprights frame. It is less than the allowable stress (173 MPa). Tab. 6 presents the maximum von Mises stress in the members of the roof structure, whereas maximum displacement are summarized in Tab. 7. All values of the modified structure are less than the allowable limits.





Loading condition	Material Member	Maximum stress [MPa] for original str.	Maximum stress [MPa] for modified str.	Allowable stress [MPa]
1	Al 6061 T6	65.4	53.2	173
	Al 2024 T3	7.1	5.9	252
	Al 7075 T651	32.2	28.1	360
	Al 2024 T351	12.2	8.2	252
2	Al 6061 T6	33.2	25.4	173
	Al 2024 T3	15.3	12.3	252
	Al 7075 T651	26.6	23.5	360
	Al 2024 T351	4.8	2.8	252
3	Al 6061 T6	75.2	53.8	173
	Al 2024 T3	31.1	27.1	252
	Al 7075 T651	35.5	28.2	360
	Al 2024 T351	11.3	8.7	252
4	Al 6061 T6	196.2	159.6	173
	Al 2024 T3	21.3	17.7	252
	Al 7075 T651	96.6	84.3	360
	Al 2024 T351	36.6	24.6	252
5	Al 6061 T6	87.2	76.0	173
	Al 2024 T3	39.5	33.5	252
	Al 7075 T651	63.3	56.2	360
	Al 2024 T351	14.2	10.1	252
6	Al 6061 T6	122.5	102.5	173
	Al 2024 T3	91.6	75.6	252
	Al 7075 T651	92.6	84.7	360
	Al 2024 T351	63.6	58.4	252

Table 6: Maximum von Mises static stress results in the members of the structure compared with the allowable limits.

Loading condition	Max. displ. [mm] for original str.	Max. displ. [mm] for modified str.	Allow. displ. [mm]
1	0.9	0.7	4
2	0.6	0.3	4
3	0.5	0.4	4
4	2.7	2.1	4
5	1.0	0.8	4
6	1.3	1.0	4

Table 7: Maximum displacement results compared with the allowable limits.

Tab. 8 presents the maximum von Mises stress under fatigue loading in the members of the modified roof module structure. All values are less than the allowable limits.



Loading condition	Maximum stress [MPa]	Allowable stress [MPa]
7	± 1.5	130
8	±21.2	130
9	69.1	130
10	37.2	130

Table 8: Maximum von Mises stress under fatigue loading compared with the allowable limits.

### BUCKLING ANALYSIS

The buckling problem is formulated as an eigenvalue problem,

$$\mathbf{K} \cdot \mathbf{q} = \lambda \cdot \mathbf{K}_\sigma \cdot \mathbf{q} \tag{1}$$

where:

$\mathbf{K}$  structural stiffness matrix,

$\mathbf{K}_\sigma$  initial stress stiffness matrix,

$\mathbf{q}$  eigenvector of displacements,

$\lambda$  eigenvalue (used to multiply the loads which generated  $\mathbf{K}_\sigma$ ).

The buckling evaluation is made of two steps: the first one, static for the given load, is used by the code to calculate the initial stress stiffness matrix of the system; the second step by means of Block Lanczos method calculates eigenvalues and eigenvectors (1) that, multiplied by the load, provide the buckling loads. The calculated static load was related to longitudinal acceleration  $g_x = 5g$  combined with vertical acceleration  $g_z = -g$ . The first three eigenvalues, are summarized in Tab. 9.

N°	Eigenvalues
1	10.106
2	10.124
3	10.126

Table 9: Buckling load eigenvalues.

Being mode one 10.106, the buckling loads of mode 1 is related to  $g_x = 50.53g$  and  $g_z = -10.106g$ . This means that the roof structure can be considered to be safe. Buckling mode shape displays are helpful in understanding how the structure is prepared to deform for buckling. Fig. 14 and 15 show the buckling mode shape for the first eigenvalue. The maximum normalized displacement is localized in a roof sheet.

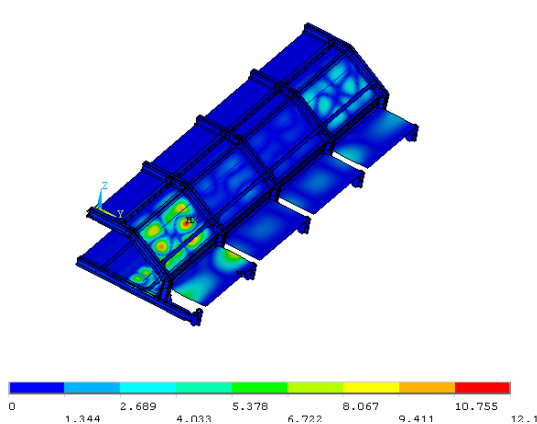


Figure 14: Buckling mode shape for the first eigenvalue.

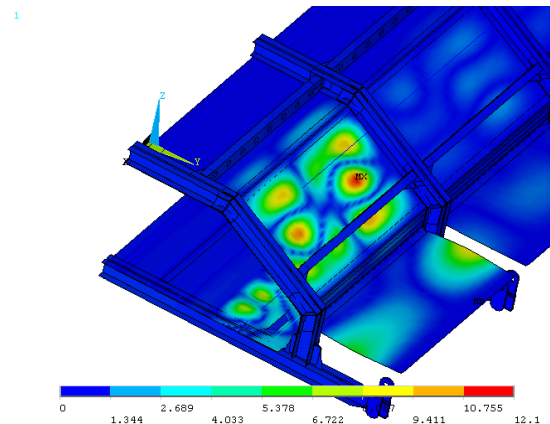


Figure 15: Buckling mode shape for the first eigenvalue (detailed view).

## VIBRATION ANALYSIS

With the growing use of advanced structures for railway vehicle design, determination of the structural dynamics characteristics is becoming increasingly important. From a space and loading perspective, it is beneficial to have the car body as long and as wide as possible, but due to the limits on the size of the car body cross-section, the structure can be rather long and slender with relatively low rigidity. A too flexible car body can lead to considerable structural deflection during travel, resulting in structural damage of it. During operation the car body is continuously excited due to the dynamic interaction between track, wheels, bogie and car body. To avoid resonances, as mentioned in [1], a common practical design rule is to keep the first natural frequency of the car body as high as possible, typically above 12 Hz.

The elastic mode shapes and modal frequencies of a railroad car, which represent its dynamics characteristics, can be evaluated by using computational methods. To determine vibrational behaviour of vehicles, normal mode or free vibration analyses, as another eigenvalue problem, are performed. Tab. 10 shows the first three frequencies of the modified roof models. The least natural frequency is 50.81 Hz that is highest of the value of 12 Hz. This means that there are not problem of resonances.

The first two elastic mode shapes of roof are shown in Fig. 16 and 17. The mode shape with the lowest frequency shows a vertical distortion of the roof structure, being the maximum normalized displacement localized in a fiberglass sheet.

N°	Frequencies [Hz]
1	50.81
2	50.84
3	51.29

Table 10: Natural frequencies of the roof module.

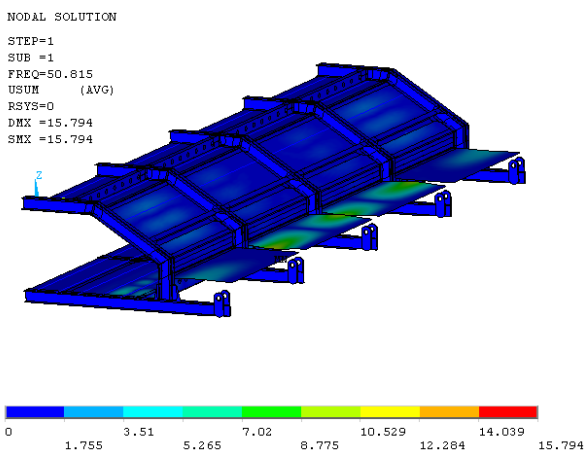


Figure 16: Elastic mode shape for the first natural frequency.

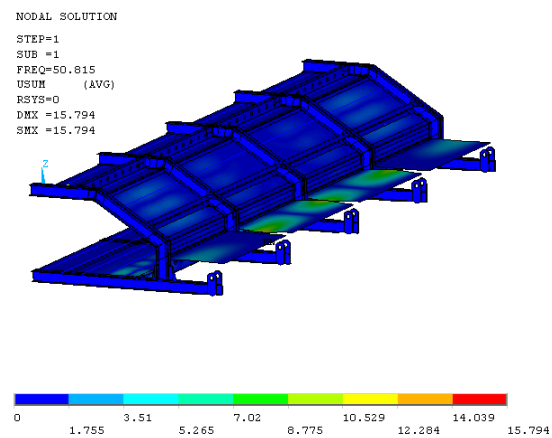


Figure 17: Elastic mode shape for the second natural frequency.

## CONCLUSIONS

In this work static, buckling and vibration behaviors of a new roof structure for a refrigerated freight car subjected to different loading scenarios as defined in standards EN 12663, UIC CODE OR 577 and ERRI B12/RP17 were studied. Using a number of numerical cases the following important conclusions are shown:

FE method is used to assess the structural behaviours of such roof structure. Three kinds of analyses were done: static analysis, linear buckling analysis and free vibrations.

Development of work and main results and conclusions are summarized as follows:

1. Two stages of static analysis are performed. In the first stage the initial concept design of roof structure was analyzed and the structural weaknesses of designs were determined. Then the structure was opportunely modified and



simulated again under the same conditions for the second stage. As a result of the modifications, the roof module structure with better static strength properties was obtained.

2. The maximum static stress in the members of the modified roof structure and relative maximum displacement are less than the prescribed allowable limits.
3. The maximum stress under fatigue loading in the members are less than the prescribed allowable limits.
4. The smallest linear buckling eigenvalues was high enough to consider adequately safe the considered roof structure.
5. The free vibration analysis shows that the first natural frequency is 50.81 Hz that is remarkably highest of the value of 12 Hz.

## REFERENCES

- [1] UNI EN 12663-1 Railway applications - Structural requirements of railway vehicle bodies - Part 1: Locomotives and passenger rolling stock (and alternative method for freight wagons). UNI, (2010).
- [2] UNI EN 12663-2 Railway applications - Structural requirements of railway vehicle bodies - Part 2: Freight wagons. UNI, (2010).
- [3] UIC leaflet 577 'Wagon Stresses' UIC, (2005).
- [4] ERRI B12/RP 17, 'Wagons', European Rail Research Institute, (1993).
- [5] Kirkpatrick, S.W., Schroeder, M., Simons, J.W., Evaluation of passenger rail vehicle crashworthiness, *International Journal of Crashworthiness*, 6(1) (2001) 95-106.
- [6] Lewis, J.H., Rasaiah, W.G., Scholes, A., Validation of Measures to Improve Rail Vehicle Crashworthiness, *Proceedings of the Institution of Mechanical Engineers, Part F: Journal of Rail and Rapid Transit*, 210 (1996) 73-85.
- [7] Hosseini-Tehrani, P., Bayat, V., Study on crashworthiness of wagon's frame under frontal impact, *International Journal of Crashworthiness*, 16(1) (2011) 25-39.
- [8] Caputo, F., Lamanna, G., Fidanza, F., Interior's safety in a regional train unit, In: 7<sup>th</sup> International Symposium on PASSIVE SAFETY 2008 Innovation in Passive Safety and Interior Design, IFV BAHNTECHNIK, (2008).
- [9] Caputo, F., Lamanna, G., Fidanza, F., Multibody investigation on the passive safety performances of seats in railway vehicles", In: *Proceedings of the 10<sup>th</sup> Biennial Conference on Engineering Systems Design and Analysis ESDA2010*, Istanbul, Turkey, (2010).
- [10] Caputo, F., Lamanna, G., Soprano, A., FE dynamic analysis of a railway seat under longitudinal impact condition, In: *Proceedings of the International Mechanical Engineering Congress & Exposition IMECE2011*, Denver, Colorado, USA, (2011).
- [11] Lamanna, G., Sepe, R., Performance evaluation of CFRP-rubber shock absorbers", In: *AIP Conference Proceedings*, 1599 (2014) 342-345.
- [12] Sepe, R., Armentani, E., Pozzi, A., Development and stress behaviour of an innovative refrigerated container with pcm for fresh and frozen goods, *Multidiscipline Modeling in Materials and Structures*, 11(2) (2015).